



International Specialty Conference on Cold-Formed Steel Structures

(1971) - 1st International Specialty Conference on Cold-Formed Steel Structures

Aug 20th, 12:00 AM

Utilization of Cold Work in Light Gage Steel

N. C. Lind

D. K. Schroff

Follow this and additional works at: <https://scholarsmine.mst.edu/isccss>



Part of the [Structural Engineering Commons](#)

Recommended Citation

Lind, N. C. and Schroff, D. K., "Utilization of Cold Work in Light Gage Steel" (1971). *International Specialty Conference on Cold-Formed Steel Structures. 2.*

<https://scholarsmine.mst.edu/isccss/1iccfss/1iccfss-session1/2>

This Article - Conference proceedings is brought to you for free and open access by Scholars' Mine. It has been accepted for inclusion in International Specialty Conference on Cold-Formed Steel Structures by an authorized administrator of Scholars' Mine. This work is protected by U. S. Copyright Law. Unauthorized use including reproduction for redistribution requires the permission of the copyright holder. For more information, please contact scholarsmine@mst.edu.

UTILIZATION OF COLD WORK
IN LIGHT GAGE STEEL

By

N.C. Lind,
Professor of Civil Engineering,
University of Waterloo,
Waterloo,
Ontario, Canada

D.K. Schroff,
Associate Programmer,
IBM Canada Limited,
36 King Street East,
Toronto 111, Canada

INTRODUCTION

Cold forming of light gage steel structural sections can modify the mechanical properties of the material significantly, generally increasing the yield strength and the ultimate strength and reducing the ductility. The modification in the cold formed regions, the "corners", is beneficial for the load carrying capacity and significant for the section as a whole, as Karren [1] has demonstrated. He has also developed an analysis to predict the increase in load carrying capacity that, with minor modifications, has been incorporated in the AISI (1968) Specification [2], in the Canadian Standard S-136 (1970) and possibly others. This analysis is workable; but it is complicated, impossible to understand without recourse to ref. [1], and very difficult to execute manually without referring to the specification or standard for details and numerical constants. The theory also assumes von Mises yield condition, and isotropic strain hardening following a power law. This complicates and specializes the analysis and is not in good agreement with material behaviour; the test results [1] show on the average a 5% difference between the yield strength in tension and compression.

It is the purpose of this paper to present a similar theory based on fewer assumptions; this analysis is considerably simplified and intuitively obvious. Specialized for a simple strain hardening law (linear) it leads to a design rule of extreme simplicity without the drawbacks mentioned above. In this rule, all aspects of material behaviour are represented through the hardening margin, $f_u - f_y$, between ultimate and yield strength, specific for the material, and a hardening constant determined empirically and taken to be the same for all materials. Because this constant is determined directly from the corner tests, rather than from stress-strain curves, it is not surprising that the results agree much better with the test data than Karren's original theory. As proposed in a draft of the CSA-S136 Standard, the rule for calculating the strength of a beam or a fully effective ($Q = 1$) column is simply to replace the yield strength by the ultimate strength over an area $5t^2$ in each 90° corner. For other corner angles the area is increased proportionally.

The theory presented by Karren had much of a semi-empirical appearance, and it was thought wise not to transgress the bounds of experimental evidence in the application, leading to the restriction in the range of corner angles (up to 120°) and the gap between yield and ultimate strengths (no less than 20% of yield). The present theory shows clearly that these restrictions can be dispensed with.

MATERIAL BEHAVIOR

The analysis requires few restrictive assumptions about the behavior of the material. For example, it is not necessary to assume that the material is isotropic or that it has equal properties in

tension and compression. It is assumed that the material is elastic-plastic; elastic strains are assumed negligible in comparison with plastic strains.

Referring to Figure 1, consider a flat element of virgin material of length h , width L and thickness t , bent by a pure uniformly distributed moment into a cylindrical shape of mean radius R (inside radius a). Because of symmetry, the coordinate axes indicate the principal directions of deformation. The element is assumed to be a contiguous part of a larger sheet that remains elastic such that its length h is unchanged in the deformation. A layer of thickness dz is therefore strained uniaxially in the process in tension or in compression depending on its position relative to the neutral surface.

The stress σ_{zz} normal to the layer is small and is neglected in the analysis. Assuming orthotropic material behavior, the principal stress directions will also coincide with the co-ordinate axes shown, such that σ_{yz} , σ_{xz} and σ_{xy} vanish. The yield condition can therefore, be described by its intersection with the two-dimensional subspace (σ_x, σ_y) of stress space (see Figure 2). In the usual fashion, strain vectors are associated with points of the yield surface; during the forming of the corner a layer of thickness dz follows the stress paths OA or OB in Fig. 2, characterized as the locus of stress points with vanishing strain in the y-direction. The engineering strain and engineering stress in this plastic deformation in the layer are denoted by e and σ respectively, related by the strain hardening law

$$\sigma = \sigma(e) \quad (1)$$

For a corner in service, on the other hand, the stresses in the plane of the cross-section are small and are neglected. The condition is one of uniaxial stress in the y-direction, represented by COD in Fig. 2. The effect of the plastic deformation is to raise the yield stress in tension and compression in the y-direction. For example, a layer compressed to point A in Fig. 2 will have yield stresses indicated by points E and C in tension and compression, respectively.

When the moments that produce the plastic deformation are released, elastic unloading takes place under plane strain conditions. If point A (Fig. 2) represents the inside corner surface ($z = t/2$ in Fig. 1), it will unload to a point such as F. The slope of AF is equal to Poisson's ratio; the precise location of F can be determined by elastic curved beam theory modified for plane strain. Curve FG indicates the locus of residual stress points for the section as a whole.

When, as in service, the corner is subsequently loaded in the axial direction, it will undergo strains of only elastic magnitude until the average stress is so high that the yield stress is developed over the entire cross section. We aim to calculate the average axial stress, which will be called the yield strength of the corner. For example, if the corner is in tension, the layer originally represented by B and G will enter a state of restrained plastic flow when point I is reached;

yielding of the corner as a whole will not occur until the material at point F reaches point H. Evidently, the pattern of yielding can be quite complicated, depending on details of the residual stress field and the location of intermediate yield surfaces. Most of the complexities of the analysis arise because the stress-strain relationship in Eq. 1 is not symmetrical with respect to the origin, as evidenced by Fig. 2 and illustrated in Fig. 3. For a given magnitude of strain, the stress value in compression is usually higher than the stress value in tension. The difference tends to increase with the strain. A consequence of this lack of symmetry is the gradual shift of the neutral axis towards the compression side; the material in the middle of the plate that is swept by the neutral axis suffers a stress reversal. The problem is also complicated by deformation of the cross-section; the distance z of a particle from the mid-surface is not conserved, as a rule. Radial expansion and contraction cause the particles of the mid-surface to move outwards relative to the surfaces of the sheet which remain approximately a distance t apart. As a consequence, the linear variation of engineering strain $e = e(z)$ with radial distance in the corner reflects a nonlinear variation of e with distance from the mid-surface. This effect could be significant when the strains are high but it is, of necessity, left out of consideration.

INFLUENCE OF STRESS-STRAIN ASYMMETRY

It will first be shown that the difference between the tension and compression segments of the stress-strain curve, Eq. 1, can normally be neglected in practice. For this purpose, let $\sigma = f(e)$ and $\sigma = g(e)$ denote the even and odd components, respectively, of the stress-strain curve as shown in Fig. 3. Let the magnitude of compressive strain on the inside surface of the corner be denoted by $c-h$ and let F denote the area under the compression stress block OC in Fig. 3. Let c denote the strain for which the area under the mean curve (OM) equals F . By a series expansion of the integral of function $f + g$ representing the compression curve:

$$\int_0^{c-h} (f+g)de = F = F - h(f+g) + \frac{1}{2} h^2 (f' + g') + \dots \quad (2)$$

Similarly, let $c + h + d$ denote the strain for which the area under the tension curve $f - g$ equals F ; then

$$\int_0^{c+h+d} (f-g)de = F = F - G + h(f-g) + \frac{1}{2} h^2 (f' - g') + \dots \quad (3)$$

in which F and G are areas as shown in Fig. 3:

$$F = \int_0^c f(e) de, \quad G = \int_0^c g(e) de. \quad (4)$$

Assume that G is small in comparison with F ; the areas in Fig. 3 then show that h and d are both small in comparison with c . Moreover, the quadratic terms in Eqs. 2 and 3 are seen to represent areas negligible in comparison with G , when the slopes f' and g' both are small (in comparison with f/c). Then, neglecting appropriate terms, these equations can be solved for the strain differences h and d to yield

$$h \approx \frac{G}{f+g}; \quad d \approx \frac{2gG}{f^2 - g^2} \quad (5)$$

Now, the true curvature k can be calculated from the strain differential over the thickness t :

$$k = \frac{(c+h+d) - [-(c-h)]}{t} = \frac{2c+d}{t} \quad (6)$$

This is the curvature corresponding to a true stress block of area F . Now, if the mean curve is used instead of the true stress-strain curves, a stress block of area F would be associated with the curvature value k^* given by

$$k^* = \frac{2c}{t} \quad (7)$$

Hence, with some rewriting

$$k = k^* \left(1 + \frac{d}{2c}\right) = k^* \left[1 + \left(\frac{G}{fc}\right) \frac{g}{f^2 - g^2}\right] \quad (8)$$

The last term in the bracket in this equation shows the relative error in substituting k^* for k . The error depends on the shape of the stress-strain curve and the value of the strain. Normally, G does not exceed twenty percent of gc and g does not exceed twenty percent of f , so that the error in k^* for a value of F is less than one percent. Inversely, the error in F for an assumed curvature will also be less than one percent, approximately, so that asymmetry in the plane strain vs. stress characteristic, $\sigma_x = f(e_x)$, can be neglected in practice:

$$f(e_x) = -f(-e_x) \quad (9)$$

Moreover, it is assumed that there exists an effective stress function and an effective strain function having the property that the plane yield stress vs. prestrain relations, $f_y^t = f_y^t(e_x)$ and $f_y^c = f_y^c(e_x)$ in the y -direction in tension and compression respectively, are affine to the stress vs. plane strain relation, $\sigma_x = f(e_x)$, in the x -direction. Thus,

$$f_y^t = Af(e_x) \quad (10)$$

$$f_y^c = Bf(e_x) \quad (11)$$

where A and B are constants.

Finally, it is assumed that the slope of the yield loci near the intersection with the σ_y -axis in Fig. 2 can be taken as constant over the range of residual stress σ_x^c and of stress σ_y of interest. These assumptions are satisfied by von Mises yield condition and isotropic work hardening, as an example.

ANALYSIS

In Fig. 4, let $\sigma = \sigma_x(z) = f(e_x(z))$, indicated by Curve 1-1, be the variation of stress in the x -direction (referred to original area of elements) through the thickness of the corner just when the last increment of plastic work in forming is performed. This stress is symmetrical with respect to the mid-surface, by Eq. 9. The corresponding yield strength variations through the thickness are indicated by the curves $f_y^t(z)$ and $f_y^c(z)$.

The presence of residual stresses after unloading should not be neglected. Curve 2-2 indicates the elastic stresses σ_x^u , induced by unloading the moments in Fig. 1, plotted such that the distance σ_x^o from 1-1 to 2-2 is the residual stress field in the x -direction. The stresses σ_x^u are distributed according to plane strain curved beam theory, modified to refer to original areas of elements. Finally, curve 3-3 indicates the residual stress in the y -direction composed of a plastic part (see path AB in Fig. 2), and an elastic part associated with the unloading and related to σ_x^u by the Poisson effect. Evidently,

$$\int \sigma_y^o(z) dz = 0 \quad (12)$$

$$\int \sigma_x^0(z) dz = 0 \quad (13)$$

where the integration extends from surface to surface.

If there were no residual stress in the x-direction, the axial force per unit arc length of corner to produce yielding in tension would be equal to the area between 3-3 and 4-4. Fig. 2 shows how the yield stress is influenced by transverse residual stress (compare KE and FB).

The deviation of the yield loci from their tangents at the points of intersection with the σ_x -axis (such as E, D, and C) for abscissas in the range of residual stress σ_x^0 is, by assumption, negligible. Also, "triangle" O550 in Fig. 4 is neglected. Then, the corner yield strength in tension, by Eqs. 10, 12 and 13 can be calculated as:

$$f_{yc}^t = \frac{1}{t} \int_{-t/2}^{t/2} (\sigma_y - \sigma_y^0) dz = \frac{1}{t} \int_{-t/2}^{t/2} [f_y^t(e_x(z)) + (f_y^t)'\sigma_x^0 - \sigma_y^0] dz$$

$$= \frac{A}{t} \int_{-t/2}^{t/2} f(e_x(z)) dz = \frac{2AR}{t} \int_0^{t/2R} f(e_x) de_x = \frac{2R}{t} AF(t/2R) \dots \quad (14)$$

in which $(f_y^t)'$ denotes the slope of the yield loci at the points on the σ_y -axis in Fig. 2, assumed to be a constant. Similarly, the corner yield strength in tension is found as:

$$f_{yc}^c = BF(t/2R)/(t/2R) \quad (15)$$

Thus, the corner yield strength is easily determined, to within a constant factor, from bend radius $R - t/2$, material thickness t , and area function $F(e)$ under the stress-strain curve (average of tension and compression). In application, the distinction between tension and compression would normally be ignored, and only tension data used. The compression yield strength would then be taken equal to the tension value.

Eq. 14 confirms intuition that the corner yield strength should be independent of the corner angle.

LINEAR HARDENING MODEL

The nine materials studied by Karren [1] showed considerable variation in general in mechanical properties, but the ultimate strain e_u was essentially constant, equal to 1/3 (variation between 0.31 and 0.40 for a 2 inch gage length). This suggests that the materials can be modelled by an ideal material hardening in tension from f_y^t to f_u^t over a strain that is the same fraction, here denoted by $3A/4\alpha$, of $e_u = 1/3$ for all the materials examined. Choosing the rigid-plastic linearly hardening material

$$\sigma = f_y + \frac{e(f_u^t - f_y^t)}{(1/3)(3A/4\alpha)} \quad (16)$$

gives the area function

$$F(e) = ef_y + \frac{2\alpha}{A} (f_u^t - f_y^t) e^2 \quad (17)$$

so that, by Eqs. 14 and 15

$$f_{yc}^t = Af_y^t + \alpha \frac{t}{R} (f_u^t - f_y^t) \quad (18)$$

$$f_{yc}^c = Bf_y^t + \alpha \frac{B}{A} \frac{t}{R} (f_u^t - f_y^t) \quad (19)$$

When no cold work is done, that is for $1/R = 0$, the yield strength Af_y^t and Bf_y^t are, respectively, equal to the virgin material yield

strength in tension, f_y^t and compression f_y^c respectively. Eqs. 18 and 19 give $B/A = f_y^c/f_y^t$ and become:

$$f_{yc}^t = f_y^t + \alpha \frac{t}{R} (f_u^t - f_y^t) = f_y^t [1 + \alpha \frac{t}{R} (\frac{f_u^t}{f_y^t} - 1)] \quad (20)$$

$$f_{yc}^c = f_y^c + \alpha \frac{t}{R} (\frac{f_y^c}{f_y^t} f_u^t - f_y^c) = f_y^c [1 + \alpha \frac{t}{R} (\frac{f_u^t}{f_y^t} - 1)] \quad (21)$$

Here, α is the only unknown quantity. Solving these equations for α and inserting the experimental values by Karren [1] shows that α ranges from 2.10 to 5.03 in tension and from 2.02 to 7.51 in compression for all the tests by Karren (totalling about 200 corners), averaging 3.34 in tension and 4.29 in compression.

This linear model permits a very simple representation for design purposes. In tension, the increment in yield force for a corner is, by Eq. 20, using the average value for α ,

$$\Delta P = (9Rt)(f_{yc}^t - f_y^t) = 9\alpha t^2 (f_u^t - f_y^t) = (\frac{\pi}{2} \frac{9}{90^\circ}) (3.34) t^2 (f_u^t - f_y^t)$$

$$\approx (5t)(t)(f_u - f_y)(9^\circ/90^\circ) \quad (22)$$

where, in the last reduction the superscript has been suppressed. We define a fictitious compressive ultimate strength as

$$f_u^c = (f_y^c/f_y^t) f_u^t \quad (23)$$

Then, Eq. (22) also will apply to the increment in yield force in compression, by Eq. 21; with α equal to 4.29, and $7t$ instead of $5t$ in the last equality.

In practice, compression data is rarely available, and it is reasonable to neglect the apparently higher hardening rate in compression. Using the value $5t$ together with tension data also in compression, Eq. (22) may be interpreted into the following simple design rule:

Cold work of a 90° corner may be taken into account by replacing the yield strength by the ultimate strength over an arc length, s , of the corner of five times the thickness. For other corner angles this arc length shall be changed in proportion to the angle.

Evidently, a difference in the value of α may be interpreted directly in terms of arc lengths. For example, if the ultimate strength is 40% higher than the yield strength, a 50% error in α is equivalent to an error of $t \times t$ in effective area of flange or cross-section. The scatter in α is therefore not so significant as it might appear at

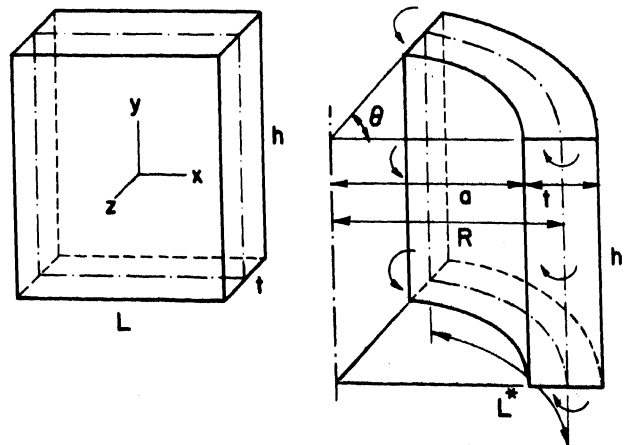


Fig. 1

first sight. There is some systematic variation, with a tendency to overestimating the strength of sharp corners. The variation could be eliminated by using a parabolic strain hardening (for example) and letting s depend on material properties, etc.

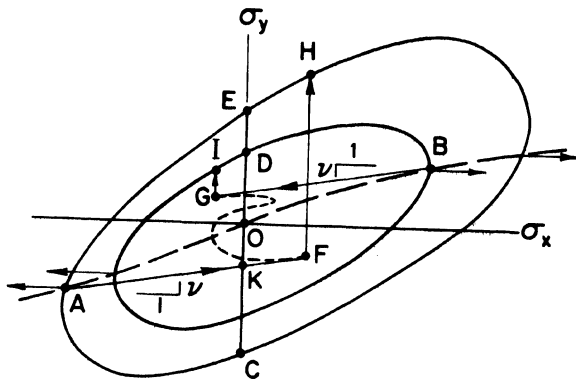


Fig. 2

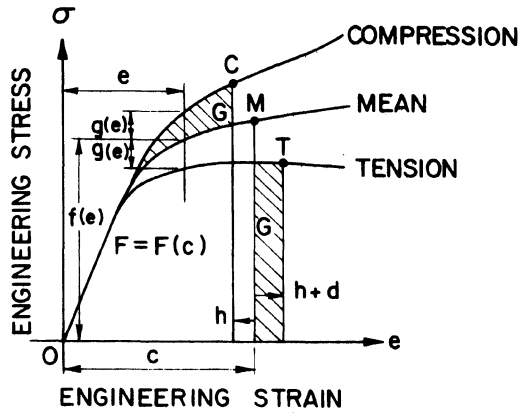


Fig. 3

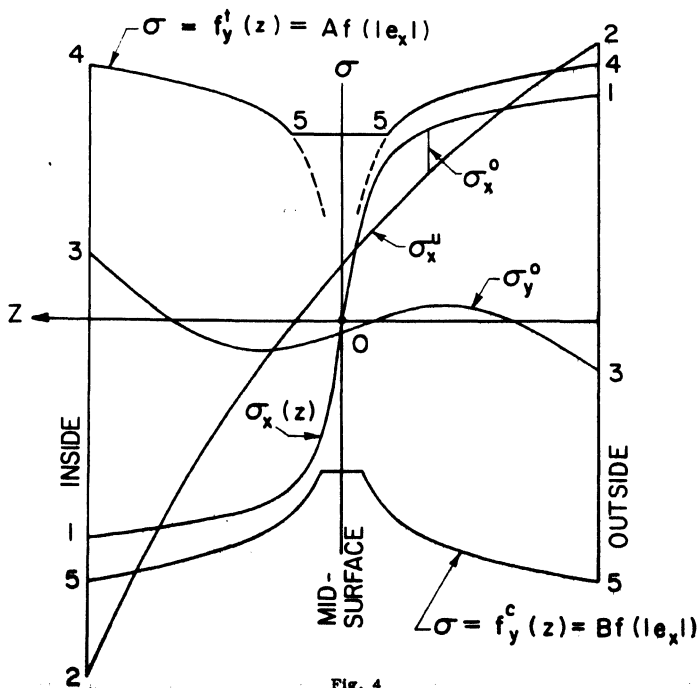


Fig. 4

CONCLUSIONS

On the basis of a simple material model and experimental data by Karren [1], it is concluded that

- (1) The raise in the yield strength of a corner depends mainly on the corner curvature ratio a/t and the area function $F(e)$ of the mean of the tension and compression stress-strain curves for the material; it is independent of the corner angle.
- (2) A linear strain-hardening model, postulating that the material is rigid-plastic and hardening from yield strength to ultimate strength over a strain of 33 1/3%, accounts for all test results available with good accuracy. By this model, the raise in yield strength depends only on a/t and the difference, $f_u - f_y$, of the ultimate strength and the yield strength.
- (3) The linear strain hardening model is convenient for design purposes. To take the cold work strengthening into account it is merely necessary to replace the yield strength by the ultimate strength at each 90° corner over an arc length of five times the material thickness. For other corner angles the arc length should be modified in proportion to the angle of bending.

ACKNOWLEDGMENTS

Thanks are due to H. Surminski and H. Sachdeva who assisted with the data analysis and programming, and to the National Research Council of Canada for financial support.

REFERENCES

1. Karren, K.W., "Corner Properties of Cold Formed Steel Shapes", Proc. ASCE, V. 92, No. ST1, Feb. 1967, pp. 401-432.
2. Specification for the Design of Cold-Formed Steel Structural Members, American Iron and Steel Institute, New York, N.Y. 1968.